Scientific Research Publishing

Open Journal of Civil Engineering, 2025, 15(3), 478-502
https://www.scirp.org/journal/ojce
ISSN Online: 2164-3172
ISSN Print: 2164-3164

Determination of the Mechanical Parameters of Dan Granite Crushed Rock for Use in Road Construction in Benin

Kocouvi Agapi Houanou*, Koutchika Roger Danvi, Kpomagbé Serge Dossou, Emmanuel Olodo

Laboratory of Energy and Applied Mechanics (LEMA), Polytechnic School of Abomey-Calavi (EPAC), University of Abomey-Calavi (UAC), Abomey-Calavi, Republic of Benin
Email: *agapikh13@yahoo.fr

How to cite this paper: Houanou, K.A., Danvi, K.R., Dossou, K.S. and Olodo, E. (2025) Determination of the Mechanical Parameters of Dan Granite Crushed Rock for Use in Road Construction in Benin. *Open Journal of Civil Engineering*, **15**, 478-502.
https://doi.org/10.4236/ojce.2025.153026

Received: July 18, 2025
Accepted: September 5, 2025
Published: September 8, 2025

Abstract

Granitic crushed materials are the most widely used materials in various fields of building and public works. These materials are more available in quantity and quality in Benin. The present study was initiated to determine the mechanical parameters of Dan 0/31.5 granitic crushed stone for use in road construction. To this end, an experimental study based on normative tests was carried out. Identification tests were carried out to determine the particle size at 80 mm and 2 mm sieves, *i.e.* 6.66% and 24.28%, the dry density, *i.e.* 2.26 t/cm^3 at a water content of 6.49% OPM, the organic matter content, 0.14%, the methylene blue value, 0.16%, the CBR index, *i.e.* 96.29% with a linear swelling of 0.07%. Micro Deval and Los Angeles values are 7.5% and 23.55% respectively. In addition, the pre-consolidation stress is 29 kPa, the compression index is 0.098% and the swelling index is 0.011%. Finally, the shear test determined the cohesion, *i.e.* 0.3 kPa, and the angle of internal friction, *i.e.*, 33.6˚. Also, based on a series of results (shear stress and horizontal displacement) from the direct shear test, the maximum shear stress and maximum shear modulus from the Hardin and Drnevich hyperbolic model, *i.e.* 349.62 kPa and 172.65 kPa, respectively. The odometer test and shear modulus were used to estimate Young's modulus, *i.e.* 274.81 MPa, and Poisson's ratio, *i.e.* 0.204. Analysis of the various results in accordance with the specifications of the CEBTP 1984 guide, revised in 2019, shows that Dan's granite crushed stone is an excellent quality road material that can be used in all pavement layers, whatever the type of pavement.

Keywords

Granite Crushed Aggregate, CBR Index, Shear Modulus, Young's Modulus, Road Material

1. Introduction

For thousands of years, mankind has used aggregates to build structures and improve the built environment. Today, with population growth and the rapid development of societies, the demand for modern infrastructure has continued to rise. This has led to ever more intensive exploitation of natural resources to meet the growing need for aggregates in road construction [1]-[4].

The West African country of Benin is undergoing rapid economic and demographic expansion. To support this economic growth and improve the quality of life of its citizens, the development of road infrastructure, public and private buildings and landscaping is a top priority for the Beninese government. In this context, Dan granite crushed stone is a strategic natural resource used extensively in road construction [4]-[6].

Given the central role played by aggregates in construction, it is imperative to master their nature and characteristics in order to guarantee the quality and durability of the works carried out. In-depth knowledge of aggregates enables their use to be optimized according to specific applications, while minimizing the risks of structural failure and guaranteeing a reduction in the environmental impacts associated with their use [1] [7].

The present study was initiated to determine the geotechnical characteristics of Dan's granite crushed stone for use in road construction. Specifically, the aim is to determine physical parameters such as grain size, density, cleanliness, organic matter content, optimum water content, sand equivalent and mechanical parameters such as CBR index, angle of internal friction, cohesion and oedometric modulus, and to determine Young's modulus and Poisson's ratio using a numerical approximation. Determining these geotechnical parameters will make it possible to assess the potential of Dan's granite crushed stone in order to define the layers of the road structure, such as the sub-base and/or base layers of flexible pavements, in which its use is possible [1] [8] [9].

2. Materials and Methods

2.1. Materials

2.1.1. Granitic Crushed Stone

Granite crushed is a material produced from granite massifs mechanically crushed into different sizes [1] [10]-[12]. The process produces sand, gravel and pebbles in a variety of angular and sharp-edged shapes. Due to its natural origin, granite crushed stone offers exceptional durability and strength.

In this study, we used 0/31.5 mm granite crushed stone from the Dan quarry in the Republic of Benin. The village of Dan is located in the commune of Djidja (Zou department), around 30 km from the commune of Bohicon in the Republic of Benin [1]. The commune of Djidja lies to the north between latitude 7˚10' and 7˚40', and to the east between longitude 1˚04' and 2˚10'. The Dan quarry is located at latitude 7˚21'44" to the north and longitude 2˚6'38" to the east. At this quarry, crushed materials are screened and stockpiled by granular class [1] [4] [13]. **Fig-**

ure 1 shows the location of the Dan quarry.

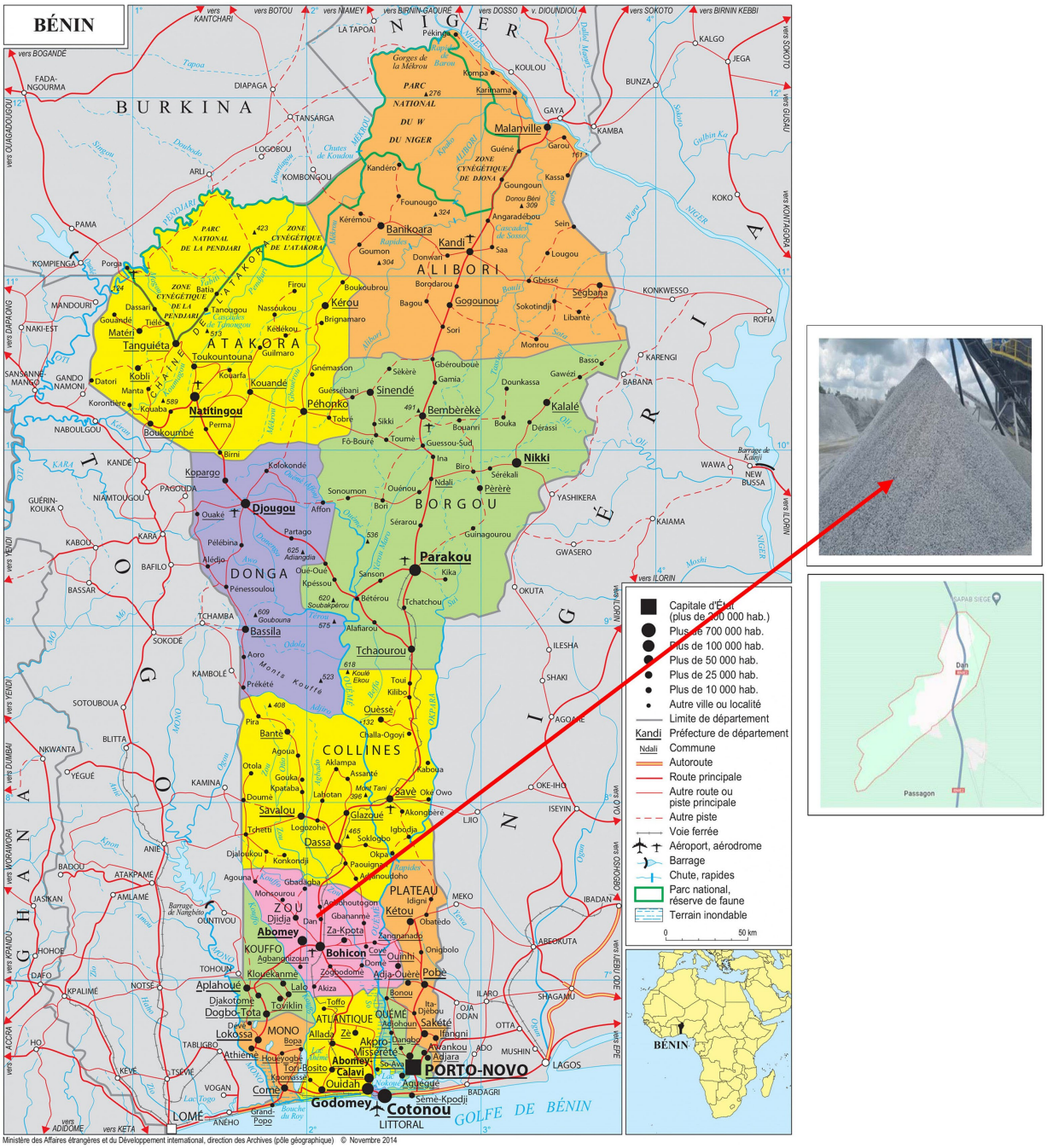

Source: https://www.worldmaps.info/maps/high/BJ/bj.jpg.

Figure 1. Location of sampling site.

2.1.2. Characterization Equipment

The equipment used for the characterization tests complies with the requirements of applicable standards in the field.

- For particle size analysis by sieving, the experimental set-up, including the accessories required to perform it, is governed by standard NF P 94-056 [14].

Figure 2 shows all of this equipment.

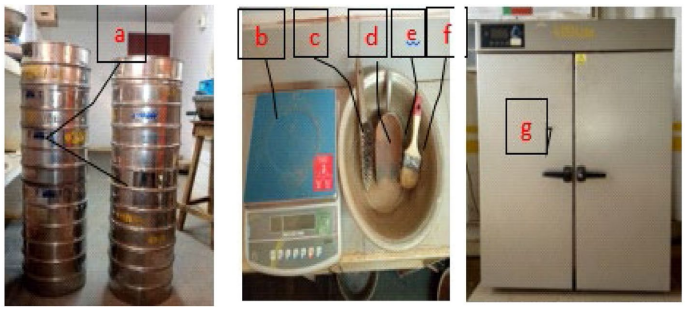

Legend:
a: Series of sieves
b: Scale of 30 kg ± 0.2 g
c: Brush
d: Scoop hand
e: Brush
f: Container
g: Oven with adjustable temperature 50˚C to 105˚C 2˚C

Figure 2. Equipment for particle size analysis.

- The experimental set-up for measuring water content by weight complies with standard NF P94-050 [15]. The equipment required is shown in Figure 3 below.

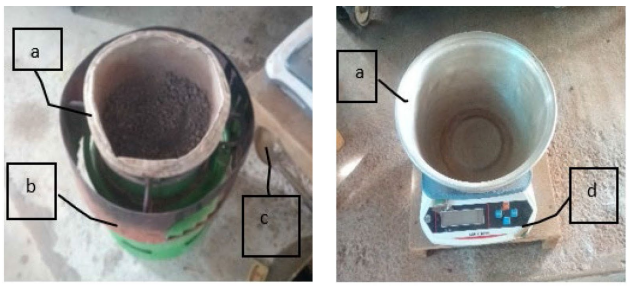

Legend:
a: Material bin
b: Gas burner
c: Ladle
d: Scale of 24 kg ± 0.2 g

Figure 3. Equipment for measuring water content.

- For the test to determine the methylene blue adsorption capacity of Dan's granite crushed stone, the experimental set-up required to perform the test is specified in standard NF P 94-068 [16]. Figure 4 below illustrates the set-up.

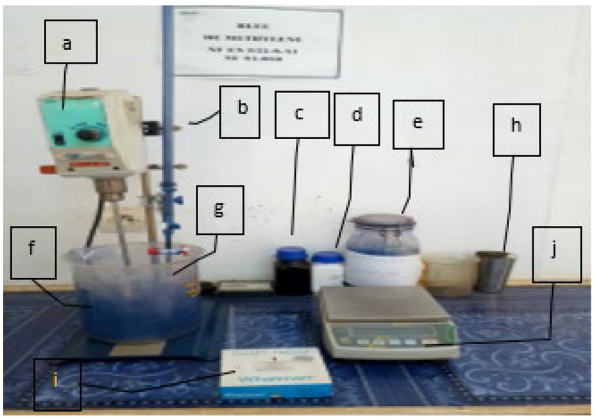

Legend:
a: Finned stirrer
b: Stand
c: Yellow glass flask
d: Dried kaolinite
e: Volumetric flask
f: Beaker
g: Burette
h: Methylene blue
i: White filter paper
j: Scale of 1000 g ± 0.1 g

Figure 4. Equipment for determining the methylene blue value.

- For the test to determine the organic matter content of Dan's granite crushed stone, the experimental set-up complies with standard XP P 94-047 [17] as shown in Figure 5 below.

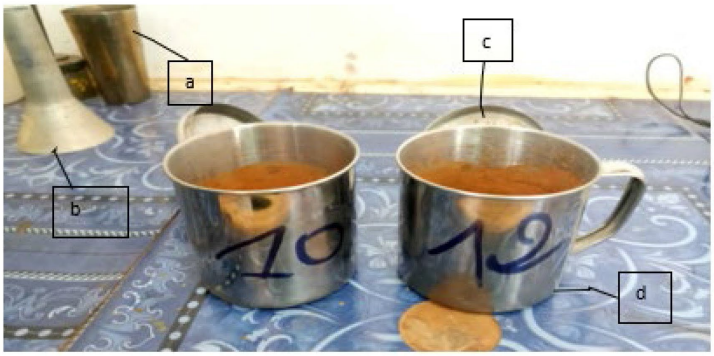

Legend:
a: Mortar
b: Pestle
c: Lid
d: Crucibles

Figure 5. Equipment for testing organic matter content.

- **Figure 6** below shows the equipment used to determine the sand equivalent in the 0/2 mm fraction of Dan granite crushed sand. This test is carried out in accordance with AASHTO T176 [18], EN 933-8 [19] and NF P18-622-8 [20].

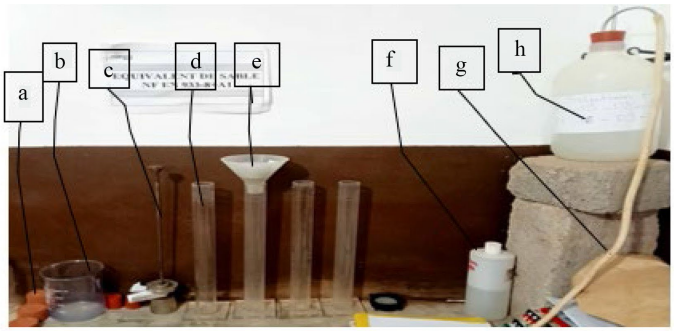

Equipment for sand equivalent determination

Mechanical stirrer

Legend:
a: rubber stoppers for test tubes.
b: beaker;
c: 1 tared piston
d: Plexiglas test tubes graduated at 100 and 380 mm
e: wide-neck funnel
f: 200 ml measuring flask.
g: 1 irrigator tube with tap and siphon.
h: 1000 ml concentrated stock solution.

Figure 6. Equipment for sand equivalent test.

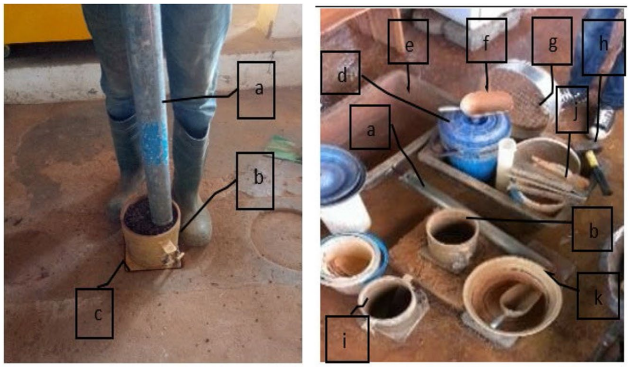

Legend:
a: Modified Dame Proctor
b: CBR mold
c: Baseplate
d: Material tray
e: Tray
f: Scoop hand
g: Sieve
h: Hammer
i: Modified Proctor mould
j: Accessories
k: Container

Figure 7. Equipment for determining compaction references.

- Figure 7 below shows a set of experimental devices for carrying out the Modified Proctor test in accordance with standard NF P94-093 [21].
- *Geotechnical testing equipment for granite crushed rock*

This section includes geotechnical testing equipment such as the CBR test, the shear test and the odometer test.

- Figure 8 below shows an experimental set-up for carrying out the CBR test in compliance with standard NF P94-078 [22].

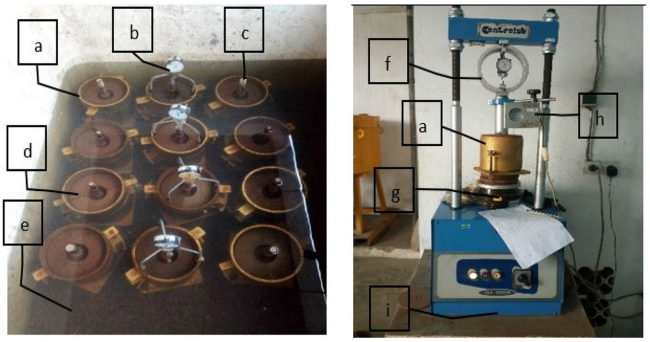

Figure 8. Equipment for determining the CBR load-bearing index

- Figure 9 shows a set of experimental devices for carrying out the rectilinear box shear test in accordance with standard NF P 94-071-1 [23] [24].

Figure 9. Direct shear test equipment.

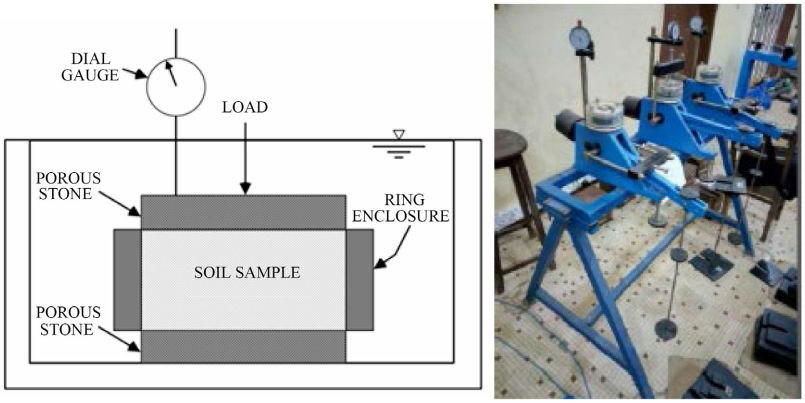

Schematic design of an oedometer (source: Boo, 2019) oedometric testing apparatus

Figure 10. Schematic design of an oedometer and oedometric testing apparatus.

- Figure 10 below shows the entire experimental device for carrying out the oedometric test according to standard XP P 94-091 [25].

2.2. Method

2.2.1. Method for Sampling Dan Granite Crushed Stone

Samples are taken in accordance with ISO 22475-1 [26].

2.2.2. Geotechnical Testing Method

The various geotechnical tests are carried out in accordance with the standards cited in §2.1.2.

Determination of the friction angle and internal cohesion by the Casagrande box shear test goes through the calibration of the raw material from the initial condition through the values obtained from the Modified Proctor test, then:

Step 1: Determination of the optimal water content and dry density on the material from the quarry (initial state).

Step 2: Determination of the optimal water content and dry density on the class 0/5 test sample.

Step 3: Carrying out the Casagrande box shears the test.

Step 4: Determination of the optimum water content and dry density on the test sample after the test.

2.2.3. Numerical Approach to Identifying the Parameters of the Hardin and Drnevich Hyperbolic Model

Previous studies have shown that the elastic behavior of soils is never linear in reality [2] [27]. Therefore, it is important to focus studies on the nonlinear behavior of soils used in road construction. To do this, several mathematical models, both hyperelastic and hypoelastic, can be used to describe these nonlinear behaviors of soils. However, it has been proven that hypoelastic models are the most recommended when it comes to small deformation studies. Two types of hypoelastic models exist, namely hyperbolic models and variable modulus models, as reported by Babaliyè in 2020. In the context of this study, hyperbolic models mathematically based on a representation of the stress-strain relationship using a hyperbolic or parabolic curve [28] are best suited to describe the nonlinear elastic behavior of soils [2] [27].

According to Hardin and Drnevich [29], the hypoelastic behavior of a material is given by Equation (1).

$$\tau = \frac{\gamma}{\frac{1}{G_{\max}} + \frac{\gamma}{\tau_{\max}}} \tag{1}$$

where $\tau_{\max}$ represents the maximum shear stress, $G_{\max}$ the maximum shear modulus, τ the shear stress and γ the shear strain.

To determine the parameters $\tau_{\max}$ and $G_{\max}$, Equation (1) was reformulated by setting: $a = 1/G_{\max}$ and $b = 1/\tau_{\max}$. This gives the following Equation (2):

$$\tau = \varphi(\gamma, a, b) = \frac{\gamma}{a + b\gamma}, a, b \in \mathbb{R} \tag{2}$$

Using a nonlinear least fit method, the parameters *a* and *b* are evaluated. This method consists of fitting the experimental data y_i to the function φ by minimizing the distance φ_i between y_i and $\varphi(\gamma,a,b)$:

$$\varphi_i = \sum_{i=1}^{n}\left[y_i - \varphi(\gamma,a,b)\right]^2 \tag{3}$$

The implementation of nonlinear regression follows the following steps:

1st Step: Linearization $\varphi(\gamma,a,b)$ of around (a_0,b_0)

$$\begin{cases}\dfrac{\partial\varphi}{\partial a}(\gamma,a,b) = -\dfrac{\gamma}{(a+b\gamma)^2}\\[2ex] \dfrac{\partial\varphi}{\partial b}(\gamma,a,b) = -\dfrac{\gamma^2}{(a+b\gamma)^2}\end{cases} \tag{4}$$

$$\varphi(\gamma,a,b) = \frac{\gamma}{a_0+\gamma b_0} - \frac{\gamma}{(a_0+b_0\gamma)^2}(a-a_0) - \frac{\gamma^2}{(a_0+b_0\gamma)^2}(b-b_0) \tag{5}$$

Let us set: $A = \dfrac{\gamma}{(a_0+b_0\gamma)^2}$; $B = \dfrac{\gamma^2}{(a_0+b_0\gamma)^2}$ and $C = \dfrac{\gamma}{a_0+b_0\gamma}$.

Equation (5) becomes:

$$\varphi(\gamma,a,b) = C - A(a-a_0) - B(b-b_0) \tag{6}$$

2nd Step: Determination of *a* and *b*.

The minimization of φ consists of canceling its first derivative with respect to the unknowns *a* and *b*. Let:

$$\begin{cases}\dfrac{\partial\varphi}{\partial a} = 0\\[2ex] \dfrac{\partial\varphi}{\partial b} = 0\end{cases} \tag{7}$$

with $\varphi(\gamma,a,b) = C - A(a-a_0) - B(b-b_0)$.

Development of the terms of the system of Equation (7).

Case of the first equation:

$$\frac{\partial\varphi_i}{\partial a} = 0 \Leftrightarrow \frac{\partial}{\partial a}\left[\sum\left(y_i - \varphi(\gamma,a,b)\right)^2\right] = 0 \tag{8}$$

$$\Leftrightarrow \sum\frac{\partial}{\partial a}\left(y_i - \varphi(\gamma,a,b)\right)\cdot\left(y_i - \varphi(\gamma,a,b)\right) = 0$$

$$\Leftrightarrow -\sum\frac{\partial}{\partial a}\varphi(\gamma,a,b)\cdot\left(y_i - \varphi(\gamma,a,b)\right) = 0$$

$$\Leftrightarrow -\sum(-A)\cdot\left(y_i - \varphi(\gamma,a,b)\right) = 0$$

$$\Leftrightarrow \sum A\left(y_i - C + A(a-a_0) + B(b-b_0)\right) = 0$$

$$\Leftrightarrow \sum Ay_i - \sum A\cdot C + \sum A^2(a-a_0) + \sum A\cdot B(b-b_0) = 0$$

$$\Leftrightarrow (a-a_0)\sum A^2 + (b-b_0)\sum A\cdot B = \sum A\cdot C - \sum Ay_i$$

$$\Leftrightarrow (a-a_0)\sum A^2 + (b-b_0)\sum A\cdot B = \sum A(C-y_i) \tag{9}$$

Case of the second equation:

$$\frac{\partial \varphi_i}{\partial b} = 0 \Leftrightarrow \frac{\partial}{\partial b}\left[\sum \left(y_i - \varphi(\gamma, a, b)\right)^2\right] = 0 \tag{10}$$

$$\Leftrightarrow \sum \frac{\partial}{\partial b}\left(y_i - \varphi(\gamma, a, b)\right)\left(y_i - \varphi(\gamma, a, b)\right) = 0$$

$$\Leftrightarrow \sum \left(-\frac{\partial}{\partial b}\varphi(\gamma, a, b)\right) \cdot \left(y_i - C + A(a - a_0) + B(b - b_0)\right) = 0$$

$$\Leftrightarrow \sum -(-B)\left(y_i - C + A(a - a_0) + B(b - b_0)\right) = 0$$

$$\Leftrightarrow \sum B\left(y_i - C + A(a - a_0) + B(b - b_0)\right) = 0$$

$$\Leftrightarrow \sum \left(By_i - B \cdot C + A \cdot B(a - a_0) + B^2(b - b_0)\right) = 0$$

$$\Leftrightarrow \sum B(y_i - C) + (a - a_0)\sum A \cdot B + (b - b_0)\sum B^2 = 0$$

$$\Leftrightarrow (a - a_0)\sum A \cdot B + (b - b_0)\sum B^2 = \sum B(C - y_i) \tag{11}$$

So we have the following system:

$$\begin{cases} (a - a_0)\sum A^2 + (b - b_0)\sum A \cdot B = \sum A(C - y_i) \\ (a - a_0)\sum A \cdot B + (b - b_0)\sum B^2 = \sum B(C - y_i) \end{cases} \tag{12}$$

Put into matrix form, the system of Equation (12) becomes:

$$\begin{pmatrix} \sum A^2 & \sum A \cdot B \\ \sum A \cdot B & \sum B^2 \end{pmatrix} \begin{pmatrix} a - a_0 \\ b - b_0 \end{pmatrix} = \begin{pmatrix} \sum A(C - y_i) \\ \sum B(C - y_i) \end{pmatrix} \tag{13}$$

Thus, the determinant (det M) of this system of equations is:

$$\det M = \begin{vmatrix} \sum A^2 & \sum A \cdot B \\ \sum A \cdot B & \sum B^2 \end{vmatrix} \tag{14}$$

$$\Leftrightarrow \det M = \sum A^2 \sum B^2 - \sum A \cdot B \sum A \cdot B \tag{15}$$

Similarly, the determinants associated with a and b are det(a) and det(b) respectively.

Either:

$$\det(a) = \begin{vmatrix} \sum A(C - y_i) & \sum A \cdot B \\ \sum B(C - y_i) & \sum B^2 \end{vmatrix} \tag{16}$$

Which is worth: $\det(a) = \sum A(C - y_i)\sum B^2 - \sum B(C - y_i)\sum A \cdot B$

So,

$$a - a_0 = \frac{\det(a)}{\det M} \tag{17}$$

That is:

$$a = a_0 + \frac{\sum A(C - y_i)\sum B^2 - \sum B(C - y_i)\sum A \cdot B}{\sum A^2 \sum B^2 - \sum A \cdot B \sum A \cdot B} \tag{18}$$

Also,

$$\det(b) = \begin{vmatrix} \sum A^2 & \sum A(C - y_i) \\ \sum A \cdot B & \sum B(C - y_i) \end{vmatrix} \tag{19}$$

which gives: $\det(b) = \sum A^2 \sum B(C - y_i) - \sum A \cdot B \sum A(C - y_i)$

So,

$$b - b_0 = \frac{\det(b)}{\det M} \tag{20}$$

Consequently,

$$b = b_0 + \frac{\sum A^2 \sum B(C - y_i) - \sum A \cdot B \sum A(C - y_i)}{\sum A^2 \sum B^2 - \sum A \cdot B \sum A \cdot B} \tag{21}$$

The following system is made up:

$$\begin{cases} a = a_0 + \dfrac{\sum A(C - y_i) \sum B^2 - \sum B(C - y_i) \sum A \cdot B}{\sum A^2 \sum B^2 - \sum A \cdot B \sum A \cdot B} \\ b = b_0 + \dfrac{\sum A^2 \sum B(C - y_i) - \sum A \cdot B \sum A(C - y_i)}{\sum A^2 \sum B^2 - \sum A \cdot B \sum A \cdot B} \end{cases} \tag{22}$$

From a Python program, the optimal value of each parameter a and b of Equation (22) is determined by respecting the stopping criterion defined by Equation (23) (Montgomery and Runger [30]; Houanou [31]; Babaliye [2]).

$$\frac{a - a_0}{a_0} < 10^{-6} \tag{23}$$

2.2.4. Evaluation of Young's Modulus (E) and Poisson's Ratio (υ)

According to Gérard Degoutte and Paul Royet [32] and Leipholz [33], the calculation of Young's modulus (E) and Poisson's ratio (υ) can be done from oedometric and shear tests. Thus, the following Equation (24) and Equation (25) are used:

$$E = 2G(1 + \upsilon) \tag{24}$$

$$E = E_{oed} \frac{(1 + \upsilon)(1 - 2\upsilon)}{1 - \upsilon} \tag{25}$$

where we denote by:

G, the shear modulus;

E, the Young's modulus;

υ, Poisson's ratio;

E_{oed}, the oedometric module.

Equation (24) and Equation (25) allowed us to obtain the following Equation (26):

$$2G(1 + \upsilon) = E_{œd} \frac{(1 + \upsilon)(1 - 2\upsilon)}{1 - \upsilon} \tag{26}$$

Thus, the transformation of Equation (26) becomes:

$$\upsilon = \frac{E_{œd} - 2G}{2(E_{œd} - G)} \tag{27}$$

Furthermore, the determination of the oedometric modulus is obtained by Equation (28):

$$E_{œd} = \frac{1 + e_0}{C_c} \frac{\sigma'_{\text{final}} - \sigma'_{\text{initial}}}{\log\left(\dfrac{\sigma'_{\text{final}}}{\sigma'_{\text{initial}}}\right)} \tag{28}$$

with

e_0 , Index of voids in the soil in place;

C_c , Compression index of the soil in place;

σ'_{initial} , Initial normal stress;

σ'_{final} , Final normal stress.

3. Results and Discussion

3.1. Results

The results of experimental tests carried out on a series of samples of Dan granite crushed rock are as follows.

3.1.1. Results of the Sieve Analysis Test

Samples from the Dan quarry were sieved for particle size analysis. The following Figure 11 and Figure 12 show the various particle size curves.

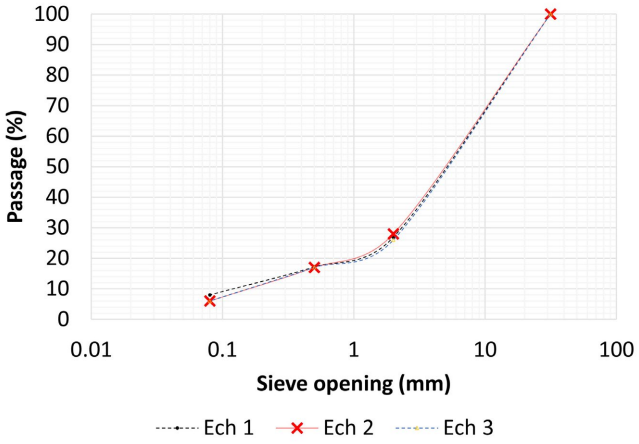

Figure 11. Granulometric curve for granitic crushed material 0/31.5.

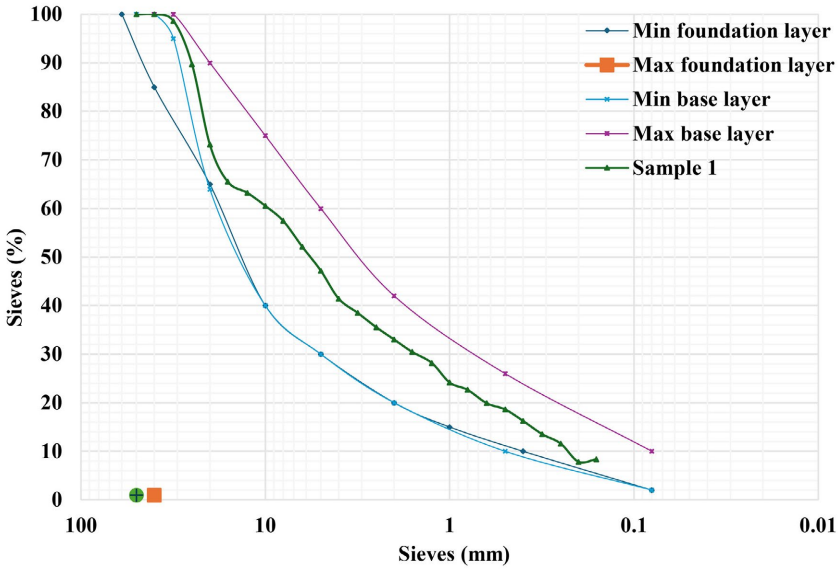

Figure 12. CEBTP limit curve for granite crushed material 0/31.5.

Key information from Figure 11 and Figure 12 is shown in Table 1 below.

Table 1. Sieving test results for granite crushed material 0/31.5.

Granulometric analysis				
Samples	$D_{(max)}$ (mm)	$C_{(2)}$ (%)	$C_{(0.5)}$ (%)	$C_{(0.08)}$ (%)
Sample 1	31.5	26.9	17.6	8
Sample 2	31.5	28	17	6
Sample 3	31.5	26	17	6
Mean	-	**26.96**	**17.2**	**6.66**
Standard deviation	-	**1.00**	**0.34**	**1.15**

We note that the curves of all three samples are within the CEBTP grading range for the sub-base layer, but not within the CEBTP grading range for the crushed materials to be used in the base layer. We note that the 0.08 sieve pass of the samples studied is less than 35%, which complies with CEBTP requirements.

The material can therefore be used as a base course. These results are similar to those found by Elenga *et al.* [34], Babaliyè [2], Houanou *et al.* [4] and Dossou [1].

3.1.2. Sand Equivalents

The results of sand equivalence values carried out on three samples made from the fine 0/2-part of 0/31.5 granitic crushed materials are presented in Table 2 below:

Table 2. Sand equivalence results for 0/2 granitic crushed material.

Designation	Sample 1	Sample 2	Sample 3	Mean	Standard deviation
ES (%)	57.00	56.00	59.00	**57.33**	**1.528**

According to these values, the sand equivalent of granitic crushed stone 0/2 is 57.33%; this sand is clean and this value is higher than the minimum 40% recommended for T3 - T4 traffic [35] [36].

3.1.3. Micro Deval Test

The results of the Micro Deval test on the three 0/31.5 granite crushed sand samples are presented in Table 3 below:

Table 3. Micro Deval results for granite crushed stone 0/31.5.

Designation	Sample 1	Sample 2	Sample 3	Mean	Standard deviation
MD (%)	7.15	7.85	8.16	**7.72**	**0.517**

From the values recorded in Table 3, it can be seen that the average value of the Micro-Deval coefficient, 7.72%, is less than 10%. This material is therefore rated as very good to good according to NF P 18-572 [37] and EN 1097-1 [38]. In accordance with the CEBTP guide [35], a mean MD coefficient, *i.e.* 7.72%, is less than 12%, so it can be concluded that the material can be used for the construction

of pavements designed for T3 - T4 traffic.

3.1.4. Los Angeles Test

The results of the Los Angeles test carried out on three samples of 0/31.5 granitic crushed stone are presented in Table 4 below:

Table 4. Los Angeles results for 0/31.5 granite crushed rock.

Designation	Sample 1	Sample 2	Sample 3	Mean	Standard deviation
Los Angeles value (%)	23	23.2	24	23.4	0.53

Analysis of Table 4 shows that, with an average Los Angeles coefficient of 23.4%, granite crushed stone offers good resistance to wear and mechanical impact. This value is less than 25% of the maximum value recommended for high-traffic wearing courses [35] [39]-[42]. It follows that this material can be used in other parts of the pavement [35] [39]-[42].

3.1.5. Measuring Methylene Blue Values

The results of the methylene blue test are shown in Table 5 below:

Table 5. Methylene blue values for 0/31.5 granite crushed material.

Designation	Sample 1	Sample 2	Sample 3	Mean	Standard deviation
VBS (%)	0.15	0.18	0.16	**0.16**	**0.01**

Analysis of Table 5 shows that the methylene blue value for granitic crushed stone 0/31.5 is 0.16%, less than 0.2%. Granitic crushed stone is therefore sandy according to standard NF P 94-068 [16].

3.1.6. Organic Matter

The results of the organic matter test are presented in Table 6 below:

Table 6. Results of organic matter test on 0/31,5 granite crushed rock.

Designation	Sample 1	Sample 2	Sample 3	Mean	Standard deviation
OM content (%)	0.10	0.15	0.18	**0.14**	**0.04**

Analysis of Table 6 shows that the organic matter content of granite crushed stone is 0.14%, less than 1%, making the material low organic [17].

3.1.7. Absolute Density

The results obtained for the density of the crushed materials are shown in Table 7 below:

Table 7. Density results for 0/31.5 crushed materials.

	Density				
Designation	**Sample 1**	**Sample 2**	**Sample 3**	**Mean**	**Standard deviation**
MV (g/cm³)	2.67	2.65	2.68	**2.67**	**0.02**

Analysis of Table 7 shows that the results for the absolute density of granitic crushed stone vary slightly between the different samples studied. The average is 2.67 g/cm³. This value indicates that the material tends to provide higher densities, which may contribute to greater strength and durability.

3.1.8. Modified Proctor Test and CBR Test

1) Modified Proctor test

The results obtained on the Modified Proctor test samples are shown in Table 8 below:

Table 8. Modified Proctor test results for 0/31.5 crushed aggregate.

Optimum Modified Proctor (OPM)					
Designation	**Sample** 1	**Sample** 2	**Sample** 3	**Mean**	**Standard deviation**
γ_{dmax} **(t/m³)**	2.37	2.24	2.19	**2.27**	**0.09**
w_{OPM} (%)	6.2	6.4	6.8	**6.47**	**0.31**

Table 8 shows the results of the Modified Proctor test carried out on 0/31.5 granitic crushed stone. The values obtained at the Modified Proctor Optimum are 2.27 t/m³ for maximum dry density and 6.47% for water content. This value shows that granitic crushed stone 0/31.5 is more compact and potentially more stable when used as backfill or pavement material [21] [35] [36] [43] [44]. Moreover, this value, similar to those obtained by Dossou [1], Houanou *et al.* [4] and Babaliyè [2], is higher than 2 t/cm³. Granite crushed stone can therefore be used in road construction to CEBTP [35] specifications in sub-base and base courses.

2) CBR test

The results of the CBR test on granitic crushed stone are shown in Table 9 below:

Table 9. CBR values for Dan granite crushed stone.

CBR load-bearing indices					
Designation	**Sample 1**	**Sample 2**	**Sample 3**	**Mean**	**Standard deviation**
100% OPM	115.50	120.10	111.25	**115.62**	**4.43**
95% OPM	98.60	102.42	87.86	**96.29**	**7.55**
90% OPM	66.55	72.66	61.50	**66.90**	**5.59**
Relative linear swelling					
95% OPM	0.056	0.067	0.082	**0.068**	**0.013**

Analysis of Table 9 shows that the CBR value for granite crushed rock at 95% OPM after immersion is 96.29%. This value is higher than 30%, which is the minimum value required by CEBTP [35], AGEROUTE-Sénégal [36] [44] for granular

materials suitable for use in sub-base courses. This material can also be used as a base course for pavements, as its CBR is higher than 80% [1] [35] [36] [43] [44]. For example, Dan's granite crushed stone can be used for both sub-base and base courses.

The relative linear swelling of this material, at 0.068%, is less than 0.5%. As a result, the material is not very sensitive to water and will exhibit very good volumetric behavior under prolonged humidity conditions [45]. It can be used as a base course, as its linear swelling is less than 1% [35] [43].

3.1.9. Direct Shear Test [23]

Table 10 gives the average values for dry density and optimum moisture content for Dan's granite crushed stone (all-material) and for the graded material before and after the shear test. These values are determined to specify the test conditions.

Table 10. Water content and dry density values on material at different stages.

Material type	Test	N°1	N°2	N°3
All materials	(%)	6.20	6.40	6.8
	$\gamma_{(d)}$ (kN/m^3)	2.37	2.24	2.19
Calibrated material	(%)	5.42	6.76	6.34
	$\gamma_{(d)}$ (kN/m^3)	1.86	1.87	1.92
Material after shear test	(%)	16.32	14.58	14.65

The values obtained enable us to plot tangential stress as a function of displacement (Figures 13(a)-(c)), and shear stress as a function of normal stress (Figures 14(a)-(c)).

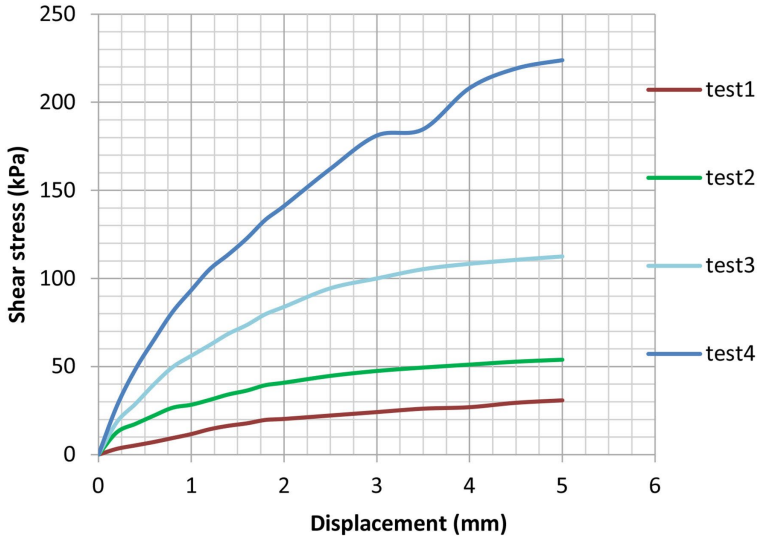

(a)

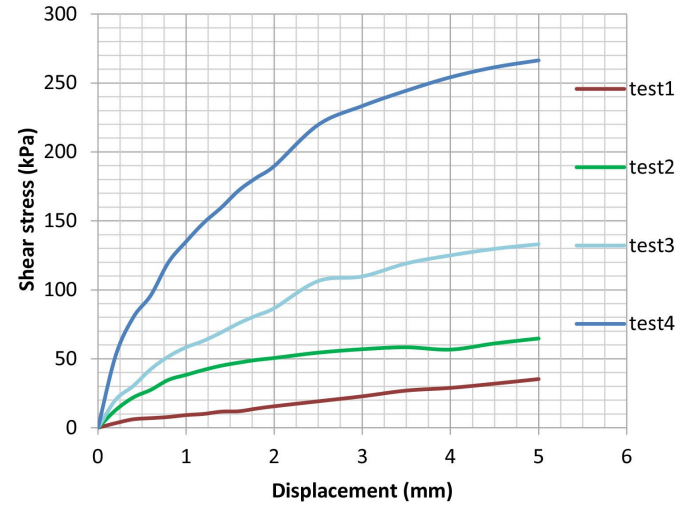

(b)

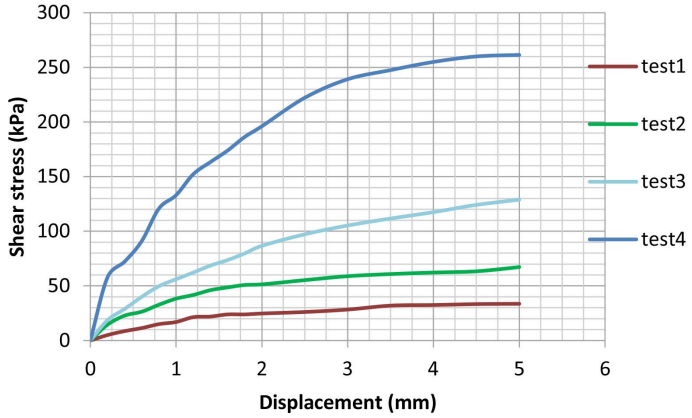

(c)

Figure 13. Shear stress vs. displacement curves. (a): Sample N˚1; (b): Sample N˚2; (c): Sample N˚3.

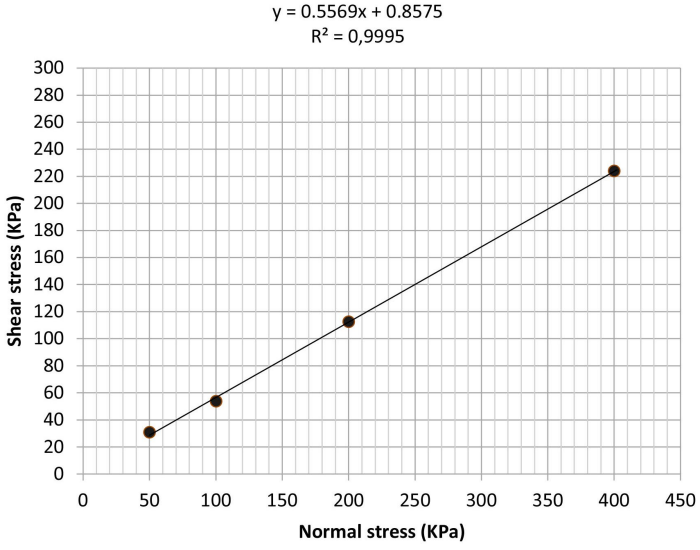

(a)

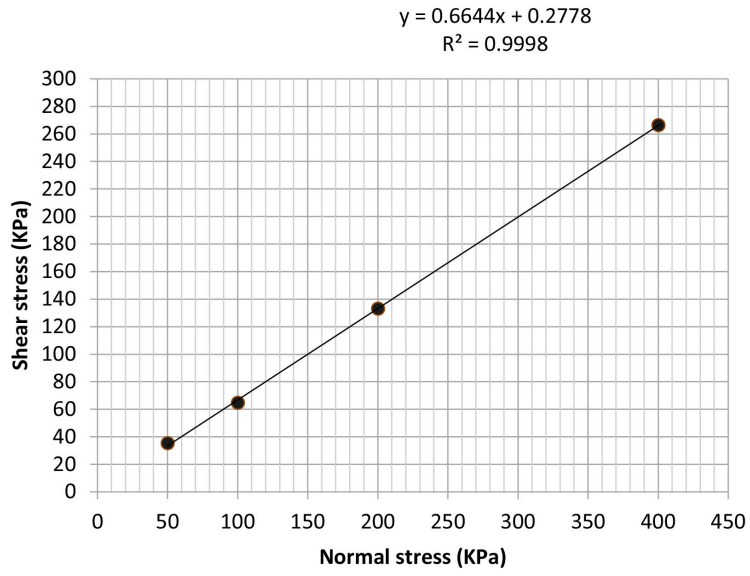

(b)

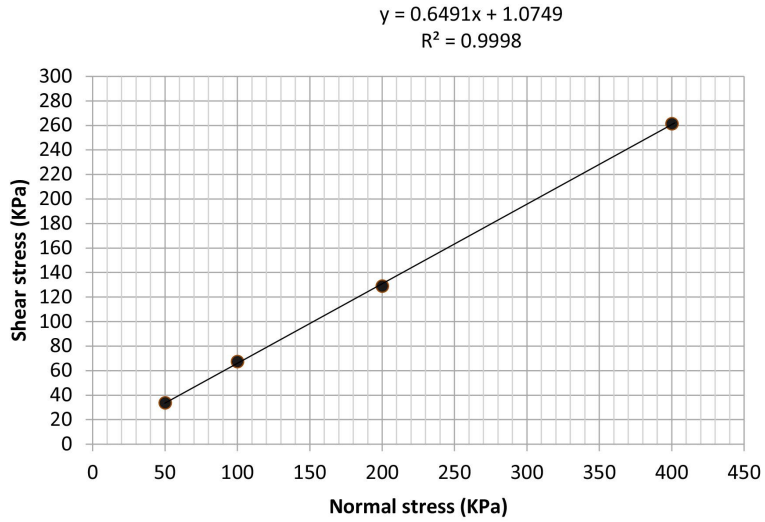

(c)

Figure 14. Shear stress vs. normal stress curve.

By identification, the equations of the straight line derived from the tests (**Figure 14**) gave the values of c and were recorded in **Table 11**.

Table 11. Shear characteristics of Dan granite crushed stone.

Designation	*c* (kPa)	(˚)
Sample 1	0.90	29.10
Sample 2	0.30	33.60
Sample 3	1.10	33.00
Mean	0.77	31.90
Standard deviation	0.42	2.44

Analysis of Figure 13 shows that shear stress evolves with increasing applied load, whatever the normal load applied.

Figure 14 shows that tangential stress evolves in the same direction as normal stress. The slope reflecting this increase is of the order of 0.60. The equation of the Coulomb line typical of a shear test is of the form:

$$\tau = c + \sigma \tan \varphi \tag{29}$$

where τ is shear stress, c cohesion, σ normal stress and φ angle of internal friction [23].

Table 11 shows that the angle of internal friction of Dan's granite crushed stone is 31.90˚, compared with 0.77 kPa for internal cohesion.

3.1.10. Oedometric Test [25]

The results of the odometer test were used to draw the following odometer curves (Figure 15):

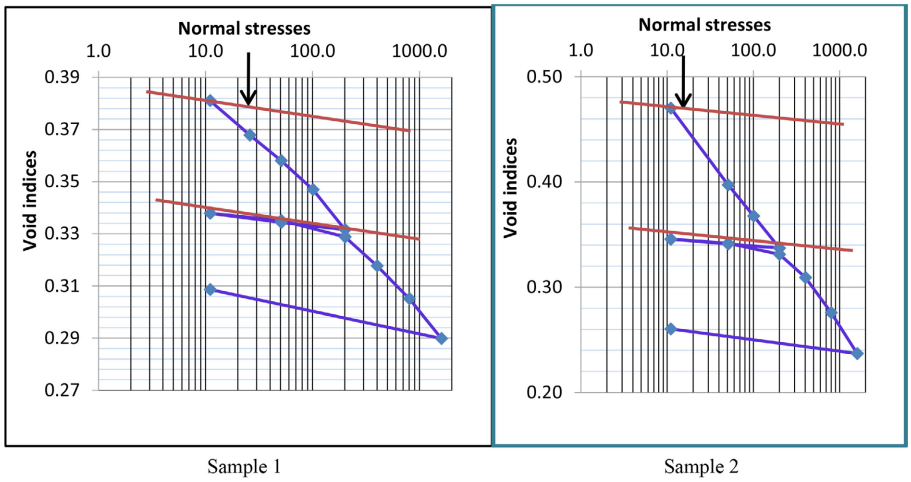

Figure 15. Oedometric compressibility curve at 95% OPM.

Table 12 shows the parameters derived from the odometer test and the corresponding curve (Figure 15).

Table 12. Average results of oedometer test carried out on granite crushed Dan specimens.

N°	e_0	$\sigma_{p(')}$ (kPa)	c_c	c_g	$\gamma_{(d)}$ (g/cm³)
Test 1	0.518	29.000	0.098	0.011	1.860
Test 2	0.420	22.00	0.0046	0.007	1.954
Test 3	0.551	27.000	0.087	0.006	1.811
Mean	0.496	28.000	0.093	0.008	1.875
Standard deviation	0.068	1.414	0.008	0.003	0.073

Analysis of Table 12 shows that the void index is 0.496, while the pre-consolidation stress is 28 kPa with a density of 1.875 g/m³. Furthermore, the coefficient

of compressibility is 0.093 while the coefficient of swelling is 0.008. It can be deduced that the material is not very compressible and does not swell [25].

Evaluation of the ratio shows that Dan's granitic crushed stone has low compressibility [46]. This may be due to its low fine particle content of 6.66%.

Also, the oedometric modulus evaluated is 295.248 MPa.

3.2. Modeling Hypoelastic Behavior

3.2.1. Development and Validation of Numerical Models

Successive iterations, based on the equation system, led to the determination of the optimal value of the Hardin Drnevich numerical model parameters. These values are presented in **Table 13** below. They concern normal stress, shear modulus and shear stress.

Table 13. Summary of optimum values for parameters G_{max} and $\tau_{(max)}$.

Normal stress (kPa)	50		100		200		400	
Parameters	G_{max}	τ_{max}	G_{max}	τ_{max}	G_{max}	τ_{max}	G_{max}	τ_{max}
Sample 1	16.650	48.128	53.212	66.923	91.027	153.629	124.331	346.826
Sample 2	9.066	149.686	78.988	74.261	81.210	200.379	220.975	352.407
Mean (kPa)	12.858	98.907	66.100	70.592	86.119	177.004	172.653	349.616

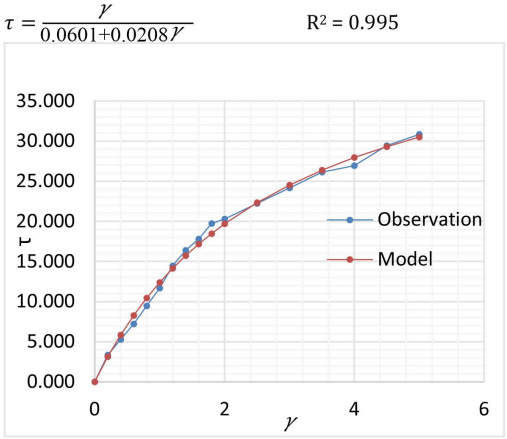

Case of 50 kPa normal stress

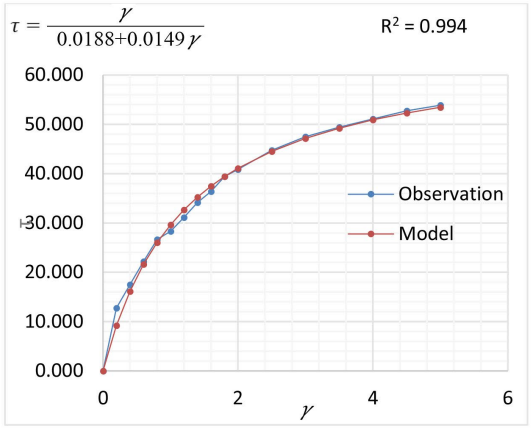

100 kPa normal stress case

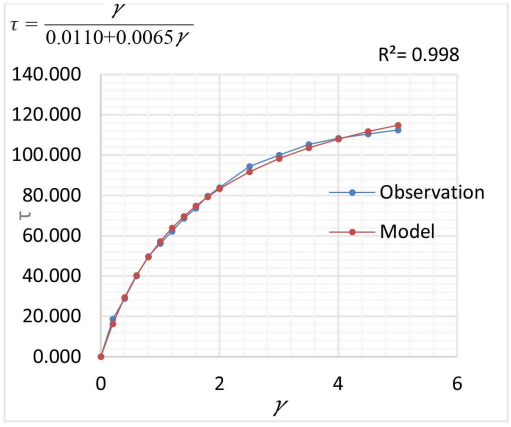

200 kPa normal stress case

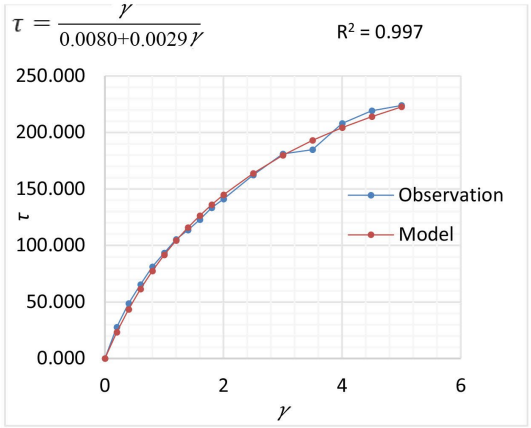

400 kPa normal stress case

(a)

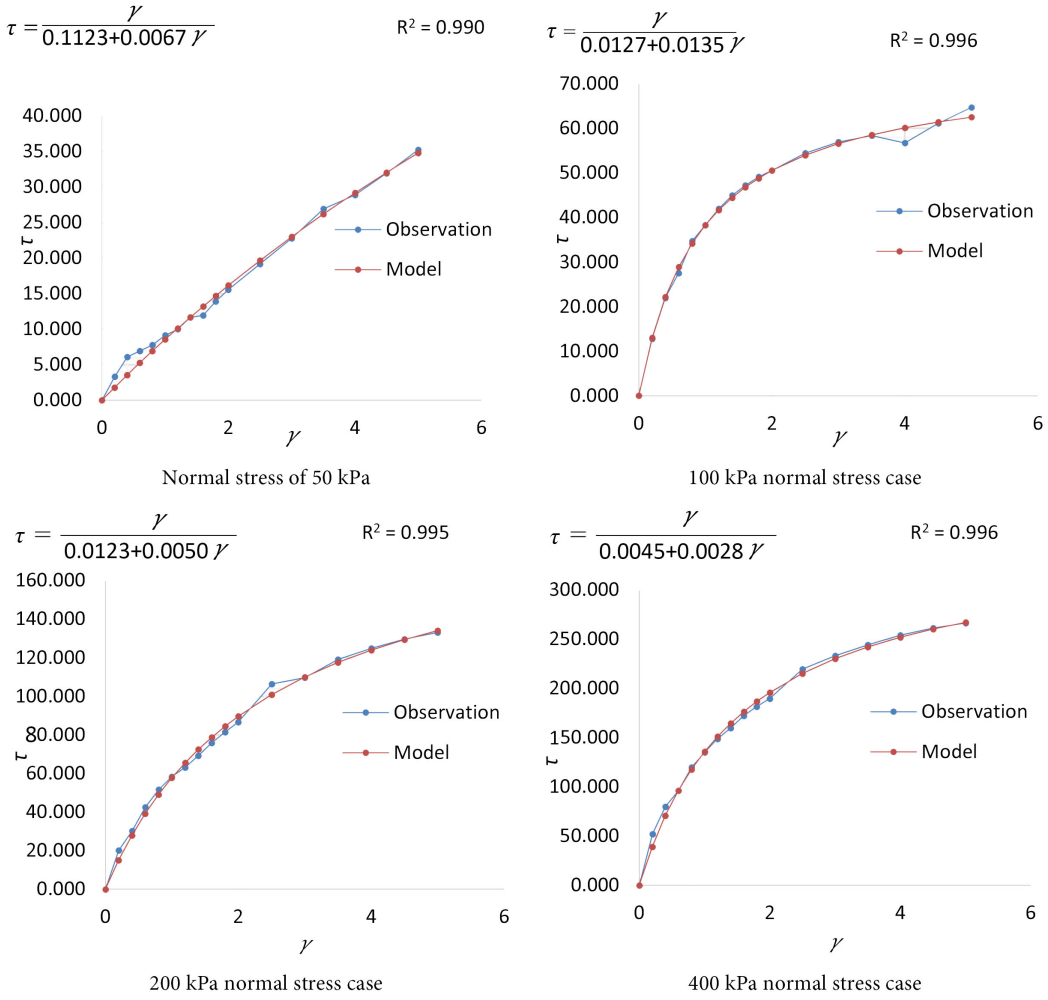

(b)

Figure 16. (a) Shear stress as a function of strain on Dan granite crushed stone (sample 1); (b) Shear stress as a function of strain on Dan granite crushed stone (sample 2).

Figure 16(a) and **Figure 16(b)** below show the Hardin and Drnevich hyperbolic behavior curves for Dan's granitic crushed stone.

It can be seen that the stress-strain curves of the model are very close to those of the observations. This means that the model fits the observations well.

The fit between the observations and the model is reflected by the coefficient of determination of each of the curves (**Figure 16(a)** and **Figure 16(b)**). **Table 14** shows the different values of the calculated coefficient of determination.

Table 14. Calculated coefficient of determination values.

Normal stress (kPa)		50	100	200	400
Sample 1	R^2 (%)	99.50	99.39	99.82	99.67
Sample 2		99.03	99.60	99.49	99.56

According to **Table 14**, the coefficients of determination of the model accord-

ing to the different compaction energies are close to 100% (ranging from 99.03 to 99.82%). This clearly shows that the Hardin and Drnevich model is adequate [1] [2] [27] [31].

3.2.2. Determination of Poisson's Ratio and Young's Modulus

Table 15 below gives the Poisson's ratios and Young's moduli derived respectively from Equations (24)-(27) and Equation (24) or Equation (25).

Table 15. Poisson's ratio and Young's modulus values for Dan granite crushed rock.

Normal stresses	$\sigma_{(n)}$ (kPa)	50	100	200	400
Maximum shear modulus	G_{max} (kPa)	12.858	66.100	86.119	172.653
Poisson's ratio	υ	0.477	0.356	0.294	0.204
Young's modulus (MPa)	E	37.988	179.233	222.893	274.808

Analysis of Table 15 shows that the shear modulus varies from 12.858 kPa to 172.653 kPa and the Poisson's ratio varies from 0.477 to 0.204, while Young's modulus varies from 37.988 MPa to 274.808 MPa. Poisson's ratio decreases with increasing normal stress. In addition, shear modulus and Young's modulus increase with normal stress at different load applications.

3.3. Discussion

Analysis of the data in Table 16 shows that the material contains little water, as its average water content of 3.5% is less than 4%. According to standard NF P 94-093 [47], this material is suitable for compaction.

Table 16. Summary of geotechnical characteristics of granitic crushed stone with respect to CEBTP 1984 thresholds, revised 2019.

Characteristics	Values for granite crushed rock	CEBTP 1984 revised 2019 thresholds	
		Foundation layer	Base layer
Percentage passing 80 µm sieve (%)	6.66		
Dry density OPM (t/m^3)	2.26	1.8 - 2.00	2.0
Linear swelling index (%)	0.07	1.00	1.00
CBR index at 95% OPM (%)	96.29	30	80
Organic matter content (%)	0.14	≤1%	≤1%
Methylene blue value (%)	0.16	0.2 - 8.0	0.2 - 8.0
Optimum water content (%)	6.66	7% and ≤13%	7% and ≤13%

Table 17 shows the result of the analysis of the characteristics of crushed granite for its use in the foundation layer according to CBTP 1984 amended 2019.

According to Table 17 above, Dan's granite crushed meets all the criteria for use as a base course for flexible pavements [35] [36] [43] [44].

Table 17. Verification of granite crushed parameters at subgrade thresholds.

Characteristics	Values for granite crushed	Thresholds CEBTP1984 revised 2019	
		Foundation layer	Conformity
Percentage passing 80 µm sieve (%)	6.66		Yes
Dry density OPM (t/m^3)	2.26	1.8 - 2.00	Yes
Linear swelling index (%)	0.07	1.00	Yes
CBR index at 95% OPM (%)	96.29	30	Yes
Organic matter content (%)	0.14	≤1%	Yes
Methylene blue value (%)	0.16	0.2 - 8.0	Yes
Optimum water content (%)	6.66	7% and ≤ 13%	Yes

Similarly, Table 18 shows the result of the analysis of the characteristics of crushed granite for its use in the foundation layer according to CBTP 1984 amended 2019.

Table 18. Verification of granite crushed parameters at base course thresholds.

Characteristics	Values for granite crushed	Thresholds CEBTP1984 revised 2019	
		Base course	Compliance
Percentage passing 80 µm sieve (%)	6.66		Yes
Dry density OPM (t/m^3)	2.26	2.0	Yes
Linear swelling index (%)	0.07	1.00	Yes
CBR index at 95% OPM (%)	96.29	80	Yes
Organic matter content (%)	0.14	≤1%	Yes
Methylene blue value (%)	0.16	0.2 - 8.0	Yes
Optimum water content (%)	6.66	7% and ≤13%	Yes

According to Table 18, Dan's granite crushed meets all the criteria for use as a base course for flexible pavements [35] [36] [43] [44]. In addition, it can be used as a reinforcement material to improve the characteristics of other materials with poor qualities [1] [35] [43].

4. Conclusions

The aim of this study was to determine the geotechnical characteristics of Dan granite crushed stone for use in road construction. Based on normative tests and in accordance with the CEBTP 1984 criteria modified in 2019, it has been shown that granite crushed Dan can be used in road construction, whatever the pavement layer. Dan granite crushed aggregate 0/31.5 has a dry density of 2.26 t/m^3 and a CBR index of 96.29% at 95% OPM. Based on direct shear tests, odometry and the Hardin Drnevich numerical model, this study determined the value of the fish

coefficient, which varies from 0.477 to 0.204.

Using the same approach, the values of the shear modulus (12.858 kPa; 66.100 kPa; 86.119 kPa; 172.653 kPa) and Young's modulus (37.988 kPa; 179.233 kPa; 222.893 kPa; 274.808 kPa) are respectively for an applied normal stress of 50 kPa, 100 kPa, 200 kPa, and 400 kPa.

The methodology used is a simple, original approach to calculating and estimating the values of certain parameters on road materials, initially taken by default in the absence of suitable equipment.

Conflicts of Interest

The authors declare no conflicts of interest regarding the publication of this paper.

References

[1] Dossou, S.K. (2023) Valorisation en technique routière de la grave latéritique de Avlamè en République du Bénin. Ph.D. Thesis, EPAC/UAC.

[2] Babaliyè, O. (2020) Comportement élastique non linéaire des mélanges de graves latéritiques et du concassé granitique non liés en couche support des chaussées souples Ph.D. Thesis, EPAC/UAC.

[3] Bohi, Z.P.B. (2008) Caractérisation des sols latéritiques utilisés en construction routière: Cas de la région de l'Agneby (Côte d'Ivoire). Ph.D. Thesis, Ecole des Ponts ParisTech. https://pastel.hal.science/pastel-00503010/

[4] Houanou, K.A., Dossou, K.S., Prodjinonto, V., Ahouétohou, P. and Olodo, E. (2022) Mechanical Characteristics of Avlamè Lateritic Gravel Improved with Granite Crushed for Its Use in Road Construction in Benin. *World Journal of Advanced Research and Reviews*, **15**, 279-292. https://doi.org/10.30574/wjarr.2022.15.2.0820

[5] Houanou, K.A., Dossou, K.S., Doko, K.V., Prodjinonto, V. and Olodo, E. (2022) Engineering Characteristics of Avlamè Lateritic Aggregate for Its Use in Road Construction in the Republic of Benin. *Australian Journal of Basic and Applied Sciences*, **16**, 8-19.

[6] Sekloka, G.H.R., Alloba, E., Houinou, G., Zinsou, L.C. and Soglo, A.B. (2015) Caractérisation des matériaux routiers et élaboration d'un catalogue pour le dimensionnement des chaussées au Sud du Bénin. Mémoire d'Ingénieur de Conception, EPAC/UAC.

[7] Houanou, K.A., Dossou, K.S. and Agbélélé, J. (2022) Optimization of the Thickness of the Subbase Layers of Flexible Pavements Based on Lateritic Gravel of Avlamè im-Proved with Granite Crushed Stone. *International Journal of Engineering Research and Science & Technology*, **18**, 19-32.

[8] Houanou, K.A., Dossou, K.S., P'kla, A., Prodjinonto, V., Adjagboni, C.E. and Olodo, E. (2022) Technical Parameters of the Cana-Atchia Lateritic Aggregate for Its Use in Road Engineering in Southern Benin. *Current Journal of Applied Science and Technology*, **41**, 21-33. https://doi.org/10.9734/cjast/2022/v41i2031746

[9] Houanou, K.A., Tchéhouali, A. and Foudjet, A.E. (2012) Identification of Rheological Parameters of the linear Viscoelastic Model of Two Species of Tropical Woods (*Tectona grandis* Lf and *Diospyros mespiliformis*). *Research Journal of Engineering Sciences*, **1**, 17-24.

[10] Agbelele, K.J., Agossou, D.Y., Houanou, K.A., Adelakoun, B.K., Ambelohoun, S.C.D.C. and Aïsse, G.G. (2023) Study of the Thermal Characteristics of a Geomaterial: Case of Savè Granites in the Republic of Benin. *Journal of Environmental Science and En-*

gineering A, **12**, 151-161. https://doi.org/10.17265/2162-5298/2023.04.004

[11] Mvindi, A.T.N. (2019) Caractérisation chimique, mineralogique et géotechnique des graveleux latéritiques d'Obala-Mbandjock (centre Cameroun) en vue de leur utilisation en construction routière. Ph.D. Thesis, Université de Yaoundé I. https://theses.hal.science/tel-03357160/

[12] Nzabakurikiza, A., Onana, V.L., Ze, A.N., Mvindi, A.T.N. and Ekodeck, G.E. (2016) Geological, Geotechnical, and Mechanical Characterization of Lateritic Gravels from Eastern Cameroon for Road Construction Purposes. *Bulletin of Engineering Geology and the Environment*, **76**, 1549-1562. https://doi.org/10.1007/s10064-016-0979-y

[13] Zomahoun, C.V., Houanou, A.K. and Vianou, C.A. (2020) Modélisation du comportement hypoélastique du mélange grave latéritique et du concassé granitique. Thèse de Master, EPAC/UAC.

[14] NFP 94-056 (1996) Sols: Reconnaissance et essais-Analyse granulométrique-Méthode par tamisage à sec après lavage. Association Française de Normalisation France.

[15] NF P94-050 (1991) Sols: Reconnaissance et essais—Détermination de la teneur en eau pondérale des sols—Méthode par étuvage. Association Française de Normalisation France.

[16] NF P94-068 (1998) Sols: Recherche et essais—Mesure de la capacité d'adsorption du bleu de méthylène d'un sol rocheux. Détermination du bleu de méthylène d'un sol par essai de déformation. AFNOR.

[17] AFNOR XP 94-047 (1998) Sols: Reconnaissance et essais—Détermination de la teneur pondérale en matières organiques d'un matériau—Méthode par calcination. Association Française de Normalisation France.

[18] AASHTO T176-16 (2016) Plastic Fines in Graded Aggregates and Soils by Use of the Sand Equivalent Test.

[19] NF EN 933-8/IN1 (2015) Essais pour déterminer les caractéristiques géométriques des granulats—Partie 8: Évaluation des fines—Équivalent de sable. AFNOR, 2.

[20] NF P18-622-8 (2015) Tests for Geometrical Properties of Aggregates—Part 8: Assessment of Fines—Sand Equivalent Test. AFNOR, 21.

[21] NF P94-093 (2014) Sols: Reconnaissance et essais—Détermination des références de compactage d'un matériau—Essai Proctor Normal—Essai Proctor modifié. AFNOR.

[22] NF P94-078 (1997) Sols: Reconnaissance et essais-Indice CBR après immersion. AFNOR.

[23] NF EN ISO 17892-10 (2018) Reconnaissance et essais géotechniques—Essais de laboratoire des sols—Partie 10: Essai de cisaillement direct. AFNOR.

[24] NF P94-071-1 (1994) Sols: Reconnaissance et essais—Essai de cisaillement rectiligne à la boîte—Partie 1: Cisaillement direct. AFNOR, 16.

[25] XP P94-091 (1995) Sols: Reconnaissance et essais—Essai de gonflement à l'œdomètre—Détermination des déformations par chargement de plusieurs éprouvettes. AFNOR, 13.

[26] ISO 22475-1 (2021) Reconnaissance et essais géotechniques—Méthodes de prélèvement et mesurages piézométriques Partie 1: Principes techniques pour le prélèvement des sols, des roches et des eaux souterraines. ISO.

[27] Babaliye, O., Houanou, K.A., Godo, A.L.A., Tchehouali, A., Vianou, A. and Foudjet A.E. (2019) Non-Linear Elastic Behavior of Lateritic Gravelly Road Material of Benin. *Journal of Materials Science & Surface Engineering*, **6**, 876-880. https://www.jmsse.in/files/655_%20Olivier%20et%20al.pdf

[28] Kondner, R.L. (1963) Hyperbolic Stress-Strain Response: Cohesive Soils. *Journal of the Soil Mechanics and Foundations Division*, **89**, 115-143. https://doi.org/10.1061/jsfeaq.0000479

[29] Hardin, B.O. and Drnevich, V.P. (1972) Shear Modulus and Damping in Soils: Design Equations and Curves. *Journal of the Soil Mechanics and Foundations Division*, **98**, 667-692. https://doi.org/10.1061/jsfeaq.0001760

[30] Montgomery, D.C. and Runger, G.C. (2003) Applied Statistics and Probability for Engineers. John Wiley & Sons.

[31] Houanou, K.A. (2014) Comportement différé du matériau bois vers une meilleure connaissance des paramètres viscoélastiques linéaires. Thèse de Doctorat, Université d'Abomey-Calavi.

[32] Poulard, C., *et al.* (2008) Gérer un projet de ralentissement dynamique. https://hal.inrae.fr/hal-02591235

[33] Leipholz, H.H.E. (1974) On Conservative Elastic Systems of the First and Second Kind. *Ingenieur-Archiv*, **43**, 255-271. https://doi.org/10.1007/bf00537215

[34] Elenga, R.G., Ahouet, L., Ngoulou, M., Bouyila, S., Dirras, G.F. and Kengué, E. (2019) Improvement of an Alluvial Gravel Geotechnical Properties with a Clayey Soil for the Road Construction. *Research Journal of Applied Sciences, Engineering and Technology*, **16**, 135-139. https://doi.org/10.19026/rjaset.16.6017

[35] Centre Expérimental de recherches et d'Etudes du Bâtiment et des Travaux Publics (CEBTP) (1984) Guide pratique de dimensionnement des chaussées pour les pays tropicaux. 2ème Edition, PARIS, 154. (La documentation française)

[36] AGEROUTE-Sénégal (2015) Catalogue de structures de chaussées neuves et guide de dimensionnement des chaussées au Sénégal. 205.

[37] NF P18-572 (1990) Granulats—Essai d'usure micro-DEVAL. AFNOR, 6.

[38] NF EN 1097-1 (2023) Essais pour déterminer les caractéristiques mécaniques et physiques des granulats—Partie 1: Détermination de la résistance à l'usure (micro-Deval). AFNOR, 24.

[39] ASTM C131/C131M-20 (2020) Standard Test Method for Resistance to Degradation of Small-Size Coarse Aggregate by Abrasion and Impact in the Los Angeles Machine. Normes Américaines, ASTM.

[40] AASHTO T 96-22 (2022) Standard Method of Test for Resistance to Degradation of Small-Size Coarse Aggregate by Abrasion and Impact in the Los Angeles Machine. ASTM C131-01.

[41] XP P94-010 (1996) Sols: Reconnaissance et essais—Glossaire géotechnique—Définitions—Notations—Symboles. Afnor.

[42] NF P18-573 (1990) Granulats—Essai de Los Angeles. AFNOR, 5.

[43] CEBTP (2019) Revue du guide pratique de dimensionnement des chaussées pour les pays tropicaux. CEBTP, 40.

[44] AGEROUTE-Sénégal (2015) Campagne de mesure de déflexion sur le réseau routier revêtue: Réflexions relatives à la définition des seuils de déflexions d1 et d2.3. 74.

[45] NF EN 13286-47 (2021) Mélanges traités et mélanges non traités aux liants hydrauliques—Partie 47: Méthodes d'essai pour la détermination de l'indice portant californien (CBR), de l'indice portant immédiat (IPI) et du gonflement linéaire. AFNOR, 14.

[46] Philipponnat, G. and Hubert, B. (2016) Fondations et ouvrages en terre. Eyrolles.

[47] NF P94-093 (1999) Sols: Reconnaissance et essais—Détermination des références de compactage d'un matériau—Essai Proctor normal—Essai Proctor Modifié. AFNOR, 20.